Compression Technique based Iris Recognition via Statistical and HOG Measures on DWT

Srinivas Halvi[1], K B Raja[2], Shanti Prasad M J[3]and Sujatha B M[4]

Abstract: An Iris recognition method is very effective in identifying human beings for several applications. We propose a Compression Technique based Iris Recognition via statistical and HOG measures on DWT in this paper. The Iris image databases viz., CASIA and UBIRIS are considered to test the algorithm by resizing them to 280x320. The Iris template of size 80x60 is extracted by considering only the horizontal portion of iris to the pupil by omitting a vertical portion of iris to the pupil to avoid occlusion above the pupil. In preprocessing Histogram Equalization (HE) is used on Iris templet to improve the eminence of the templet. The two Level Discrete Wavelet Transform (DWT) is operated to compress Iris templet by considering only the LL band for the extraction of features. The statistical measures such as Mean, Variance and Standard Deviation (SD) and also Histogram of Gradients (HOG) are computed from the LL band of the DWT. The final features are obtained by concatenating statistical parameters and HOG coefficients. The test and database images are related through final features using Euclidian Distance (ED) to test the performance of the projected method. It is witnessed that the performance of the projected technique is improved related to the current approaches.

Index Terms: Biometrics, DWT, Face Recognition, Image processing, Statistical measures

1 INTRODUCTION

Identity recognition is very important and tedious with the advent of information technology. Old-fashioned documentation procedures, which include password, identity card and so on; do not meet the requirement of the present world with the defect of easy to forge, hack and lose. In recent years, biometric identification has become a popular topic with the benefits of being steady, suitable and easy to integrate with a computer for protection, watching and controlling systems to achieve automatic management. The biometrics includes physical traits viz., face, fingerprint, iris, palmprint and behavioral traits such as voice, handwritten signature, keystroke. The prominent benefit of biometric validation is that it cannot be misplaced or disremembered as an individual should be present during the documentation process [1]. It was reported that the iris configurations are distinctive and constant to individual and could serve as humanoid identification by Flom and AranSafir [2] in the 1980s makes use of many mathematical design recognition methods on images of one or two of the iris of human eyes. The arbitrariness of iris form has great dimensionality, which makes recognition results with high-level confidence to support rapid and reliable thorough searches.

[1]*Department of Medical Electronics, Dayananda Sagar College of Engineering, VTU, Bangalore, India, srinivas.halvi65@gmail.com*
[2]*Department of ECE, University Visvesvaraya College of Engineering, Bangalore University, Bangalore, India, raja_kb@yahoo.com*
[3] *Department of ECE, K.S. Institute of Technology, VTU, Bangalore, India.*
[4]*Dept. of ECE, Acharya Institute of Technology, VTU, Bangalore, India,*

The eye images are captured and the iris templet is extracted from each eye image and computing performance parameters
which results in iris recognition [3]. Over the last decades, researchers have introduced many iris recognition techniques [4]
in which two primary classification methods such as statistical and learning-based approaches are projected. In the statistical method, some important features from the iris templet are extracted and compared with the distance factor to access and discover its nearby match. The examples of the feature extraction techniques are Principal Component Analysis (PCA) [5], Wavelet [6], Curvelet [7], Gabor filter [8] and non-orthogonal transform [9]. Learning built approaches, practice one or additional statistical-based feature extraction systems. The classifiers viz., Neural Networks [9] or Support Vector Machine [10] are used for the matching. PCA technique is widely used for dimensionality cut in features along with both statistical and learning-centered procedures.

Contribution: In this paper, compression based Iris Recognition via statistical and HOG measures on DWT is proposed. The HE and DWT are used in pre-processing to improve the excellence of an Iris template and compress the size of iris templet. The statistical parameters and HOG coefficients are computed from the LL band for initial features. The final features obtained by concatenating statistical and HOG coefficients. The database and test features are related to computing performance parameters using ED.

Organization: The research paper is organized as follows: Section 2 enlightens the literature survey of existing research; the projected Iris recognition model is pronounced in Section 3; Section 4 labels the proposed algorithm. Section 5 enlightens the experimental results; Section 6 deliberate the conclusion

2 LITERATURE SURVEY

The existing iris recognition techniques presented by various researchers based on preprocessing, feature extraction and matching are explained in this section. Ahmad Ghaffariet al., [11] projected Intensity Separation Curvelet based PCA(ISC-PCA) iris recognition. The Canny Edge detection and Hough transform techniques are used on eye image to extract the iris part and converted into rectangular depiction. The HE technique on iris image is used to rise the accuracy and contrast of an image and then used Fast Digital Curvelet Transform (FDCT). It divides the image into sub-bands and the sub-band coefficients with same level are concatenated to create two matrices for co-efficient in each level. A single 2D matrix is generated when the co-efficient matrices within each frame is vectored and combined. PCA is applied on 2D matrix to extract its Eigen vectors. The Euclidean distance is used to measure the nearness of different iris images. The result on the images of CASIA-Iris-Interval image datasheet shows ISC-PCA outperforms the other learning based methods. The ISC-PCA significantly uses less computation cost and ISC-PCA has increased performance when compared with other methods.

Wei Zhang et al., [12] projected a network model which uses eye image dissection to precisely locate the iris area. Many researches in the recent years applied deep learning theory to the iris segmentation [13]- [17]. Convolutional Neural Network(CNN) is a network arrangement in deep learning that used to fragment the iris which in turn decreases the number of iris features and feature collection to enhance the precision of the segmentation. The noisy iris images attained with lengthy distance and in motion are used in this method. Liu et al., [18] presented Hierarchical Convolutional Neural Network (HCNN) and Multi-Scale Fully Convolution Network(MFCN). Kuo Wang and Ajay Kumar [19] presented an approach of dilated convolutional kernel and residual learning in the framework for extra precise iris matching. The architecture of the deep neural network is also simplified. The problem of unintentional pupil dilation and scale changes throughout the iris imaging establish the main basis for the Iris deformation which was addressed in the work. Eduardo Ribeiro et al., [20] presented CNN with diverse deep learning methods to recover the texture and adequate grained facts from the low resolution images. The different architectures with and without image re-projection were tested to reduce the artifacts using on dissimilar iris databases to confirm the feasibility of CNN for iris super resolution. The post processing step of CNNs result is called image re-projection [21] to rise the resolution of NIR and mobile phone iris images. Later the outcomes are compared via superiority valuation algorithms and recognition approaches with two classical methods [22] as well as with PCA method. The CNN reconstruction method improves the result in the recognition background for dissimilar scaling issues comprising very little resolution images.

3 PROPOSED IRIS RECOGNITION METHOD:

The efficient iris recognition system is developed to identify persons by extracting compressed iris portion and features are extracted using statistical and HOG techniques are displayed in Figure 1

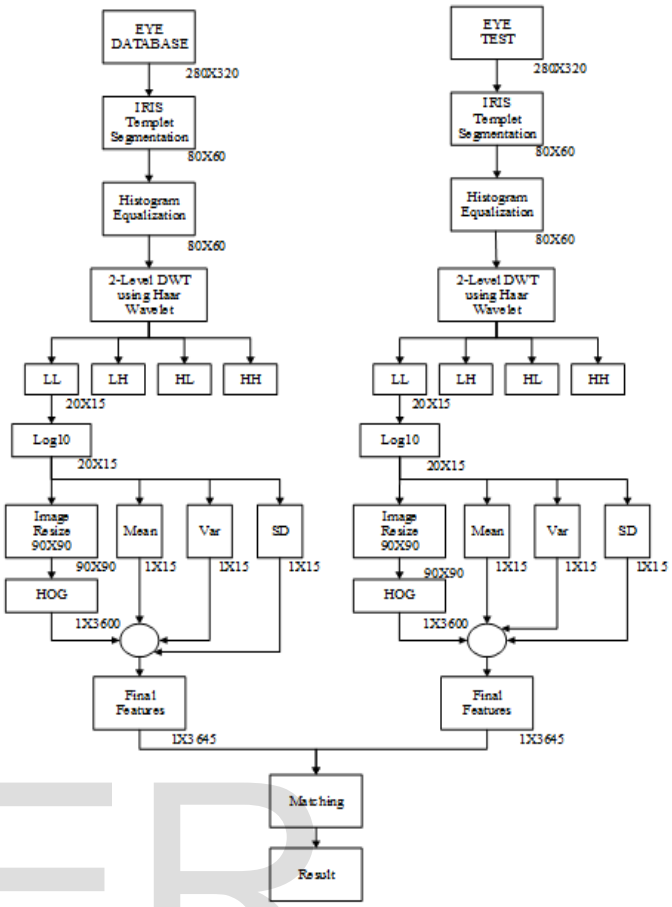

Fig.1. Flow chart of projected method

3.1 Eye Image Database:

The iris is a circular area sandwiched in the middle of sclera and pupil with distinctive features. The Chinese Academy of Sciences Institute of Automation (CASIA V.I) iris database [23] is considered to experiment with the projected system. The database comprises of 756 eye images of 108 persons with seven images per person. The size of each eye image is 280x320 with a grayscale. The eye images of every person were captured in two sessions, in the first session first three images and in the second session four images. The eye images were captured in an extremely controlled atmosphere. They exhibit homogeneous appearances and their noise factors are solely associated with obstructions of eyelids and eyelashes as shown in Figure 2.

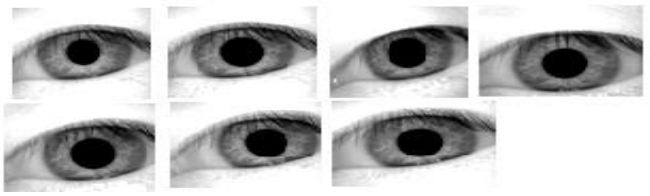

Fig 2: Eye image Samples of single person

3.2 Iris Pattern Extraction: The iris part is extracted from an eye image by removing the pupil and sclera.

3.2.1 Recognition of Pupil: The iris is in the middle of the outer borderline of the pupil and the innermost borderline of the sclera. The blackest area in an eye image is the pupil portion and is approached with appropriate intensity edge values. The pixels of similar intensity values are grouped based on connected component analysis and morphological processes to find the center and boundary of a pupil. The pupil is recognized by setting suitable threshold values to differentiate between pupil and iris part as shown in Figure 3.

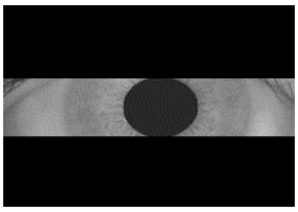

Fig 3: Pupil with Iris boundary

3.2.2 Iris templet: The horizontal left and right side boundary of the pupil is extracted that gives iris. The analysis of the CASIA iris database [24] estimates that the iris radius varies between 90 and 125 from the center of the pupil. The horizontal left and right side iris portions of forty-five pixels from the boundary of the pupil are considered to form an iris template. The portion of iris above the pupil is detached by means of morphological processes to exclude eyelid and eyelashes as shown in Figure 4 a. The fragments of iris to the left and right side of pupil boundary are measured to create an iris template through a resize of 60*80 as shown in Figure 4 b.

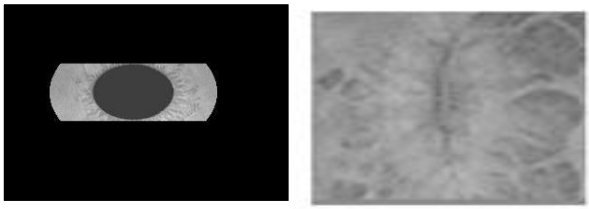

(a) Horizontal Iris Portion (b) Template of Iris

Fig4: Iris Template Extraction

3.3 Histogram Equalization:

It is an image contrast enrichment method based on pixel intensity values [25]. It rises the contrast of image through equally dispensing all pixels of an image equally over the complete intensity range using a probability density function of pixel intensity values. The probability density function gives the probability of occurrence of a number of pixels with particular intensity in an image. The iris templet and its corresponding histogram equalized iris templet are shown in Figure 5. The pattern of iris templet is clearly visible after Histogram Equalization.

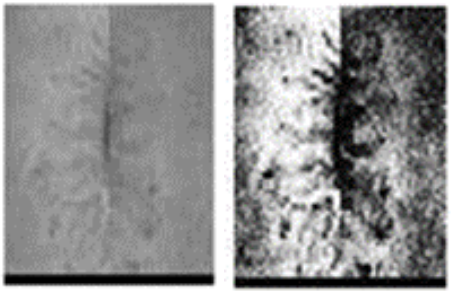

(a) Iris Templet (b) HE Iris Templet

Fig 5. Histogram Equalization Effect

3.4 Discrete Wavelet Transforms (DWT) [26]: The wavelets are discretely sampled and capable of capturing both frequency and time domain information in wavelet transform. It decomposes the image into four sub-bands based on the combination of filters and scaling filters. The 2D-DWT is engaged on the rows and columns of original HE iris templet by using both low and high pass filters simultaneously and sampled by factor 2 in digital image processing to generate four sub-bands. At every decomposition level of DWT, four sub-images corresponding's to four sub-bands such as approximated image (LL band), vertical (LH), horizontal (HL) and diagonal (HH) are obtained. The LL band corresponding to the low-frequency band consists of substantial information of HE iris templet. The three other bands viz., LH, HL, and HH are corresponding to high-frequency bands consists of vertical, horizontal and diagonal edge data that are unimportant in nature. The two-level DWT is applied to HE iris templet to generate four sub-bands. The HE iris templet and its corresponding four bands of DWT are as shown in Figure 6. The compressed LL band image is considered for further processing to extract features using HOG and statistical measures.

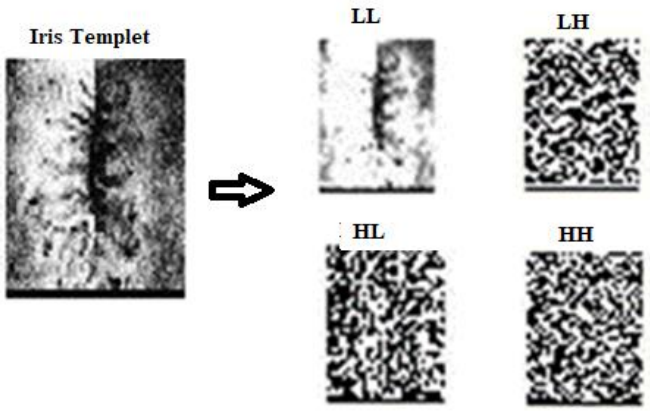

Fig 6. DWT Decomposition

3.5 Statistical Measures [27]: The arithmetic mean, variance and standard deviation measures are used to compute statistical measures on LL sub-band iris templet of DWT to extract statistical features. The definitions of statistical metrics are as follows

3.5.1 Arithmetic Mean (AM): It is the average value of samples and is usually denoted by $\bar{x}$ is given in equation 1

$$\bar{x} = \frac{1}{n}\sum_{i=1}^{n} x_i \qquad (1)$$

Where x_i = The values of coefficients

n = Number of coefficients

Example: - Consider 2X2 matrix m

$$m = \begin{bmatrix} 50 & 170 \\ 120 & 132 \end{bmatrix}$$

Convert matrix into row vector

$$v = [50 \quad 170 \quad 120 \quad 132]$$

$$\bar{x} = \frac{50 + 170 + 120 + 132}{4}$$

$\bar{x}$ =118

3.5.2 Variance: It is the squared deviation of each coefficient from the mean of the row vector and is given in equation 2

$$variance = \frac{1}{n}\sum_{i=1}^{n}(x_i - \bar{x})^2 \text{----------(2)}$$

$$= \frac{1}{4}[(50-118)^2 + (170-118)^2 + (120-118)^2 + (132-118)^2]$$

=1882

3.5.3 Standard Deviation (σ):.5

$$\sigma = \sqrt{variance}$$

$$= \sqrt{1882}$$

= 43.38

3.6 Histogram of Oriented Gradients (HOG): It is extensively used in image detection by computing and counting histograms of gradient directions in confined regions of images [28], and the magnitude and directions of gradients are used as features. The gradient magnitudes are large around edges and corners as it contains usually more data about object shape than the flat region. The HOG is used on the resized LL band matrix of DWT to obtain initial features. The horizontal and vertical kernels shown in Figure 7 are used to find horizontal and vertical gradients to estimate the histogram of gradients.

$$Horizontal\ Kernal\ Filter = \begin{bmatrix} -1 & 0 & 1 \end{bmatrix}$$

$$Vertical\ Kernal\ Filter = \begin{bmatrix} -1 \\ 0 \\ 1 \end{bmatrix}$$

Fig. 7. Kernel filters for horizontal and vertical gradients

The gradients comprise of magnitude and direction of each pixel values that are computed through Equations (3) and (4). The magnitude of gradient is large wherever there is a severe variation in intensity of the adjacent pixels.

(3) $Magnitude = \sqrt{g_H^2 + g_V^2}$

(4) $Direction\ (angle) = arctan\left(\frac{g_V}{g_H}\right)$

where g_H is horizontal gradient and g_V is vertical gradient.

The LL band matrix is fragmented into numerous blocks with four cells in each block and every cell comprises 8X8 pixels. The histogram of gradients for every cell is calculated and scattered onto nine bins of a histogram with angles 0 to 180 degrees. The range of 20 degrees is assigned to each bin. A bin is nominated based on the direction obtained from Equation (4) then the magnitude values each pixel is assigned to the corresponding bin which is obtained from Equation (3). The illustration of the bin selection of histogram and transfer of magnitudes is shown in Figure 8.

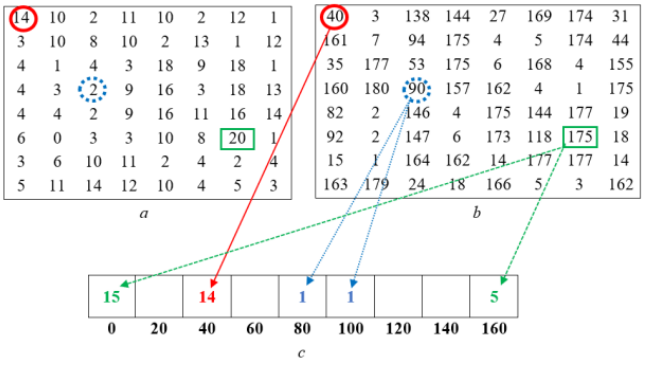

Fig. 8. The illustration for bins selection of histogram in each cell (a) Magnitudes, (b) Direction, (c)Nine Bins Histogram of Gradients

The magnitudes, directions and nine bin histogram of gradients of 8X8 cells of resized LL band matrix and allotment of angles to bins are shown in figure 8. The nine bin histogram of gradients having 9 slots with each slot of 20 degrees. The resized LL band matrix of size 90X90 is segmented into 8X8 cells and HOG is used on each cell to get nine HOG coefficients.

The magnitude 14 from Figure 8(a) corresponding to a direction of 40 degrees from Figure 8(b) is transferred to the 3rd bin of Figure 8(c). The magnitude 2 corresponding's to a direction of 90 degrees are transferred to bins of 80 degrees and 100 degrees equally as 90 degrees' bin is not available. Similarly, magnitude 20 corresponding to a direction of 175 degrees is transferred to 160 degrees and 0 degrees with a ratio of 1/4 and 3/4 of magnitude i.e., the magnitude 5 to 160 degrees and 15 to 0 degree. The four neighbouring cells of size 8X8 are clustered into one chunk of size 16X16. The thirty-six HOG coefficients are obtained for every 16X16 chunk. The final features of the resized LL band matrix are computed by considering a 50% overlap of each chunk. The entire number of overlapped chunks is 10X10 in the resized LL band matrix that generates final features of 10X10X36 = 3600.

4 PROPOSED ALGORITHM:

Compression Technique based Iris recognition using statistical and HOG measures on DWT to detect human beings efficiently is adapted in the projected algorithm is given in Table 1.

Problem Definition: Human beings are recognized efficiently using the concatenation of statistical measures and HOG coefficients for final features being adapted in the proposed method. The novel concept of HOG coefficients and statistical measures on LL band of two-level DWT is introduced to obtain better results with the following objectives:

1. To increase Recognition Rate.
2. To decrease the error rate.

Table 1 Proposed Algorithm to recognise human beings

Input: Eye images of standard databases Output: Identification of human beings with a low error rate. 1. The eye images from CASIA and UBIRIS databases are considered to experiment with the proposed algorithm. 2. The Iris templet is extracted by considering only the horizontal portion near the pupil and discarding the vertical portion near the pupil. 3. The contrast of iris templet is enhanced using the HE technique. 4. The two-level DWT decomposition is applied on HE Iris templet to consider a corrupted version of the LL band for further processing. 5. The log-10 is used on LL band coefficients to convert coefficients into moderate values. 6. The statistical measures such as AM, variance, and SD are used to create the first set of features. 7. The LL band is resized to 90x90 and the HOG technique is used to creäte the second set of features. 8. The two sets of features are concatenated to create final features. 9. The final features of the test and database Iris templets are related to ED to examine the performance of the proposed method.

5. PERFORMANCE EXAMINATION:

The descriptions of performance evaluation factors, the performance evaluation of the projected technique using CASIA and the UBIRIS iris database for diverse mixtures of PID and POD and comparison of the projected method with present methods are discussed in this section.

5.1 Definitions of Performance Evaluation Parameters: The parameters such as False Recognition Rate (FRR), False Accept Rate (FAR), Equal Error Rate (EER), Optimum Recognition Rate (ORR), and Maximum Recognition Rate (MRR) are computed based on the following equations to test the proposed method.

5.1.1 False Recognition Rate (FRR): It is defined as the number of authentic persons in the database are rejected as imposters as given in equation 1

$$FRR = \frac{Number\ of\ authentic\ persons\ rejected}{\text{Total number of persons in PID}} \quad \text{---------- (1)}$$

5.1.2 False Accept Rate (FAR): It is defined as the number of imposters accepted as authentic persons and is computed using equation 2

$$FAR = \frac{Number\ of\ persons\ from\ outside\ database\ accepted\ as\ authentic\ persons}{\text{Total number of persons in POD}} \quad \text{----------(2)}$$

5.1.3 Equal Error Rate (EER): It is the optimum error corresponding to optimum threshold value where the values of FRR and FAR becomes equal.

5.1.4 Maximum Recognition Rate (MRR): It is defined as the maximum number of persons recognized correctly and is given in equation 3

$$MRR = \frac{Total\ number\ of\ authentic\ persons\ recognised\ correctly}{\text{Total number of persons in PID}} \quad \text{----------(3)}$$

5.1.5 Optimum Recognition Rate (ORR): It is defined as the value of recognition rate at optimum value of threshold.

5.2 Performance Evaluation: The Iris databases such as CASIA and UBIRIS are used to assess the performance of the projected technique by computing performance parameters.

5.2.1. Result analysis using CASIA Iris database: The performance of the projected technique is examined with parameters such as EER, ORR, MRR by varying PID values keeping POD values constant are given in Table 2. The EER values increase and ORR values decrease with an increase in PIDs between 20 and 70 for the POD value of 30. The MRR values are constant at 100% for variations in PID's.

Table 2: Performance variations on CASIA database

PID	POD	% EER	% ORR	% MRR
20	30	0	100	100
30	30	4	96	100
40	30	4	96	100
50	30	4	96	100
60	30	7	93	100
70	30	8	92	100

The deviations in the values of FRR, FAR, and TSR through threshold variations with PID and POD combination of 70 and 30 is as shown in Figure 9. The values of FRR decrease as the values of threshold increase, and FAR values increase with increase in threshold values. The TSR values varies between zero and 100% as threshold values lies between zero and one. The percentage EER is 8 and OOR is 92 at optimum threshold value of 0.66. The value of recognition rate reaches maximum 100% from threshold values 0.67.

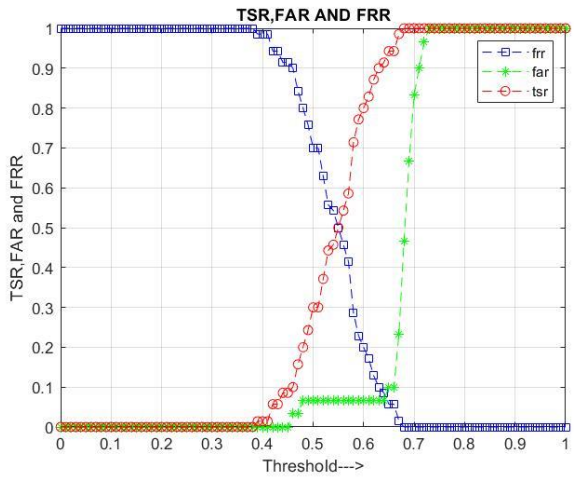

Fig. 9. Performance parameters Vs threshold values with70 in PID and 30 in POD

The values of percentage EER, ORR, and MRR for variations in POD with constant PID are shown in Table 3. The values of EER, ORR and MRR are constants at 4, 96 and 100 for PID of 30 and variations of POD's between 20 and 70. It is noticed that, the performance evaluation parameters are independent of variations in POD's and depends on variations in PID's. The percentage MRR for entire amalgamations of PID and POD's are 100. The maximum percentage of ORR is 100 with20 in PID and 30 in POD combination, and minimum percentage of ORR is 92 with 70 in PID and 30 in POD combination.

Table 3: Performance variations with constant PID using CASIA database

PID	POD	%EER	%ORR	%MRR
30	20	4	96	100
30	30	4	96	100
30	40	4	96	100
30	50	4	96	100
30	60	4	96	100
30	70	4	96	100

5.2.2 Result Analysis using UBIRIS Database: The evaluation parameters are calculated for diverse amalgamations of PID and POD's to verify the performance of the projected method is given in Table 4. It is witnessed that, the percentage EER values rises by increase in the values of PID. The percentage ORR values decreases through increase in PID's for constant POD value and percentage MRR values remain constant at 90 for all amalgamations of PID and POD's.

Table 4: Performance variations with constant POD using UBIRIS database

PID	POD	%EER	%ORR	%MRR
30	30	10	86.67	90
50	30	18	81	90
70	30	20	76	90

The deviations of FRR, FAR, and TSR with variations in threshold values for PID and POD combinations of 70 and 30 is as shown in Figure 10. The percentage FRR values decreases from 100 to zero for rise in threshold values. The percentage values of FAR and TSR varies from zero to 100 and 90 respectively for increase in threshold from zero to one.

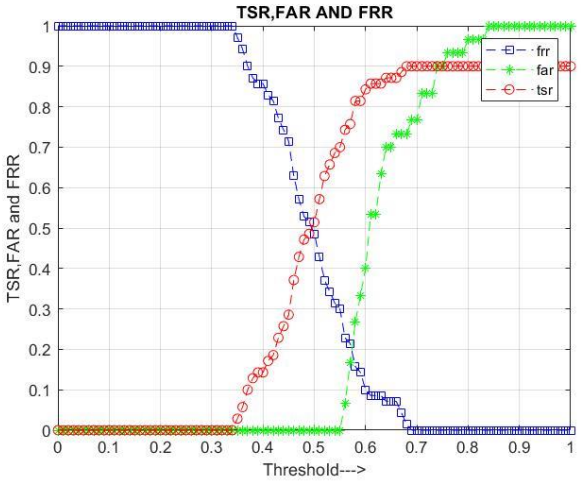

-

Fig. 10. Performance parameters Vs threshold values with 70 in PID and 30 in POD

The deviations of percentage EER, ORR and MRR for dissimilar values of POD keeping PID constant as shown in Table 5. It is noted that, the percentage values of EER, ORR, and MRR remains constant at 10, 86.67 and 90 for variations in POD's between 30 and 70 with constant PID at 30.

Table 5: Performance variations with constant PID using UBIRIS database

PID	POD	%EER	%ORR	%MRR
30	30	10	86.67	90
30	50	10	86.67	90
30	70	10	86.67	90

5.3 PROJECTED METHOD COMPARISON WITH EXISTING TECHNIQUES:

The proposed method is compared with the current methods presented by Rangaswamy and Raja [29], Wang Anna et al., [30], Conti et al., [31] and Ruihui et al., [32] on the premise of using same CASIA iris database.

Table 6: Comparison results on CASIA Iris database

Authors	Techniques	% Recognition Rate
Rangaswamy and Raja [29]	AHE+HE+Gabor+FFT	90.2
Wang Anna et al.,[30]	WNN+WPNN	94.5
Conti et al.,[31]	Micro-Features	95.5
Ruihui Zhu et al.,[32]	SIFT	90.0
Proposed Method	Statistical measures+ DWT	96.0

The percentage recognition rate is improved in the case of projected method with minimum of 0.5% and maximum of 5.8% as shown in Table 6. Hence it is evident that the projected method using HE and DWT in preprocessing to enhance iris templet quality and feature extraction by the combination of statistical and HOG measures gives better result compared to existing methods.

6 CONCLUSION: The patterns of the iris are distinctive to every individual and are the most effective physiological biometrics to recognize a person. Compression based Iris Recognition using statistical and HOG measures on DWT is proposed for the identification of persons in this paper. The Iris templet is extracted by omitting a vertical portion of iris above pupil to obtain a compressed area of iris. The HE is considered to improve the superiority of iris templet and then DWT is used to generate compressed LL band coefficients in preprocessing operation. The initial features are extracted using statistical parameters and HOG coefficients. The statistical and HOG measurements are concatenated to get final features. The ED used to compute the performance parameters of the projected method by comparing database and test features. The experimental result shows that the performance of the projected method is enhanced than the present approaches. In future Neutral Network or Support Vector machine is used in place of ED to improve the performance of the projected technique.

REFERENCE:

[1] J. Daugman, "How Iris Recognition Works", *IEEE Transaction on Circuit and Systems for Video Technology*, Vol.14, No.1, pp 21-30, January 2004.

[2] L. Flom and A. Safir, "Iris recognition system," *US Patent US4 641 349A*, February, 1987. [Online]. Available: https://patents.google.com/patent/US4641349A/en

[3] V. Nazmdeh, S. Mortazavi, D. Tajeddin, H. Nazmdeh, and M. M. Asem, "Iris Recognition; From Classic to Modern Approaches," *IEEE Annual Computing and Communication Workshop and Conference (CCWC)*, pp. 981–988, January 2019.

[4] Yasir A. Jasim, Ayad A. Al-Ani, and Laith A. Al-Ani "Iris Recognition using Principal Component Analysis," *IEEE International Conference on Information and Sciences*, pp 89-95, November 2018.

[5] T. TzeWeng Ng, Thien Lang Tay, and Siak Wang Khor "Iris Recognition using Rapid Haar Wavelet Decomposition," *IEEE International Conference on Signal Processing Systems,* vol. 1, pp. V1820–823, July 2010.

[6] H. Guesmi, H. Trichili, A. M. Alimi, and B. Solaiman, "Iris Verification System based on Curvelet Transform," *IEEE International Conference on Cognitive Informatics and Cognitive Computing*, pp. 226–229, August 2012.

[7] Ritesh Vyas, TirupathirajuKanumuri and GyanendraSheoran, "Iris Recognition using 2-D Gabor Filter and XOR-SUM Code," *IEEE India International Conference on Information Processing*, pp. 1–5, August 2016.

[8] C. Chou, S. Shih, W. Chen, V. W. Cheng, and D. Chen, "Non-Orthogonal View Iris Recognition System," *IEEE Transactions on Circuits and Systems for Video Technology*, vol. 20, no. 3, pp. 417–430, March 2010.

[9] Kamal Hajaria, UjwallaGawandeb, and YogeshGolhar, "Neural Network Approach to Iris Recognition in Noisy Environment," *Elsevier Procedia Computer Science International Conference on Information Security & Privacy*, vol. 78, pp. 675–682, January 2016

[10] Sushilkumar S. Salve1, and S. P. Narote, "Iris recognition using SVM and ANN," *International Conference on Wireless Communications, Signal Processing and Networking*, pp. 474–478, March 2016.

[11] Ahmad Ghaffari, Matthew Zarachoff, Akbar Sheikh-Akbari and EbrahimShaghoui, "Intensity Separation based Iris Recognition Method using Curvelets and PCA," *IEEE Mediterranean Conference on Embedded Computing*, June 2019.

[12] Wei Zhang, Xiaoqi Lu, Yu Gu, Yang Liu, XianjingMeng and Jing Li, "A Robust Iris Segmentation Scheme Based on Improved U-Net," *IEEE Access*, vol.7, pp. 85082-85089, June 2019.

[13] Nianfeng Liu, Haiqing Li, Man Zhang, Jing Liu, Zhenan Sun, and Tieniu Tan, "Accurate Iris Segmentation in Non-Cooperative Environments Using Fully Convolutional Networks," *IEEE. International Conference on Biometrics (ICB)*, pp. 1-8, June 2016.

[14] E.Jalilian and A.Uhl, "Iris Segmentation using Fully Convolutional Encoder Decoder Networks," *Springer Deep Learning for Biometrics*, pp. 133-155, August 2017.

[15] Y.Yang, P.Shen and C.Chen, "A Robust Iris Segmentation using Fully Convolutional Network With Dilated Convolutions," *IEEE International Symposium on Multimedia*, pp. 9-16, December 2018.

[16] Ying Chen, Wenyuan Wang, Zhuang ZengandYerong Wang, "An Adaptive CNNs Technology for Robust Iris Segmentation," *IEEE Access*, vol.7, pp.64517-64532, May 2019.

[17] G.Huang, Z.Liu, L.van der Maaten,and K. Q.Weinberger, "Densely Connected Convolutional Networks," *IEEE Conference on Computer Vision and Pattern Recognition*, pp. 2261-2269, 2017.

[18] N. Liu, H. Li, M. Zhang, J. Liu, Z. Sun, and T. Tan, "Accurate Iris Segmentation in Non-Cooperative Environments using Fully Convolutional Networks," *IEEE International Conference on Biometrics*, pp. 1-8, June 2016.

[19] Kuo Wang and Ajay Kumar, "Toward More Accurate Iris Recognition using Dilated Residual Features," *IEEE Transactions on Information Forensics and Security*, vol.14, no.12, pp.3233-3245, December 2019.

[20] Eduardo Ribeiro, Andreas Uhl and Fernando Alonso-Fernandez,"Super-Resolution And Image Re-Projection for Iris Recognition," *IEEE International Conference on Identity, Security and Behavior Analysis*, 2019.

[21] H. Y. Chen and S. Y.Chien, "Eigen-Patch: Position-Patch Based Face Hallucinationu Eigen Transformation," *IEEE International Conference on Multimedia and Expo*, pp 1–6, July 2014.

[22] F. Alonso-Fernandez, R. A. Farrugia, and J. Bigun, "Learning-Based Local-Patch Resolution Reconstruction of Iris Smart Phone Images," *IEEE/IAPR International Joint Conference on Biometrics,* IJCB, October 2017.

[23] http://www.sinobiometrics.com, Chinese Academy of Sciences Institute of Automation. CASIA iris image database 2004.

[24] http://www.springerimages.com, Springer Analysis of CASIA Database.

[25] M. Abdullah-Al-Wadud, Md. H. Kabir, M. A. A. D and O. Chae. "A Dynamic Histogram Equalization for Image Contrast Enhancement", *IEEE Transactions on Consumer Electron,* vol. 53, no. 2, pp. 593–600, 2007.

[26] Mallat, S. G. "A Theory for Multiresolution Signal Decomposition: The Wavelet Representation," *IEEE Transactions on Pattern Analysis and Machine Intelligence,* Vol. 11, Issue 7, pp. 674–693, July 1989.

[27] https://www.sciencedirect.com/topics/economics-econometrics-and-finance/statistical-measures

[28] N. Dalal and B. Triggs, "Histograms of Oriented Gradients for Human Detection", *IEEE International Conference on Computer Vision and Pattern Recognition*, vol. 1, pp. 886-893, 2005

[29] Rangaswamy Y and K B Raja, "Iris Recognition based on Translation of Iris Templates, AHE, HE and Gabor Wavelet Filter," *International Journal of Computer Science and Network,* vol. 5, no. 5, pp. 842-853, October 2016

[30] Wang Anna,ChenYu, Wujie and Zhangxinhua, "Iris Recognition Based on wavelet Transform and Neural Network," *IEEE International Conference on Complex Medical Engineering,* pp.758-761, May 2007

[31] V. Conti, G. Milici, F. Sorbello and S.Vitabile, "A Novel Iris Recognition System Based on MicroFeatures," *IEEE Workshop on Automatic Identification Advanced Technologies*, pp.253-258, June 2007.

[32] Ruihui Zhu, Jinfeng Yang and Renbiao Wu, "Iris Recognition Based on Local Feature Point Matching," *IEEE International Symposium on Communications and Information Technologies*, pp.451-454, October 2006